Structure and Magnetic Alignment of Metalloporphyrazine Columnar Aggregates in Their Mesophases and Crystalline Phases†

Brian D. Pate,‡ Sung-Min Choi,§,|| Ulrike Werner-Zwanziger,‡ David V. Baxter,⊥ Jeffrey M. Zaleski,*,‡ and Malcolm H. Chisholm*,#

Departments of Chemistry and Physics, Indiana University, 800 East Kirkwood Avenue, Bloomington, Indiana 47405, Department of Nuclear and Quantum Engineering, Korea Advanced Institute of Science and Technology, Daejon 305-401, Republic of Korea, National Institute of Standards and Technology, Gaithersburg, Maryland 20899, and Department of Chemistry, The Ohio State University, 100 West 18th Avenue, Columbus, Ohio 43210

Received April 26, 2001. Revised Manuscript Received December 31, 2001

The response of a series of metalloporphyrazine liquid crystals to external magnetic fields has been investigated. Small-angle neutron scattering (SANS) data of the octa(*n*-decylthio)-porphyrazine complexes of the diamagnetic late first-row transition elements (Ni, Zn) reveal a perpendicular orientation of the columnar directors with respect to applied magnetic fields as low as 0.50 T when the samples are cooled from their isotropic phases. The threshold aligning field for the analogous cobalt derivative is half that of the diamagnetic complexes, while the copper porphyrazine exhibits no preferred alignment at fields as high as 1.02 T. We account for these observations on the basis of the competing diamagnetic and paramagnetic moments of the complexes. Correlated solid state and mesophase ^{13}C NMR studies on the nickel and zinc complexes indicate time-averaged disk tilt angles of 27° with respect to the columnar directors in the liquid-crystalline phase.

Introduction

While all current commercial applications of liquid-crystalline materials employ organic calamitics, recent studies of metallomesogens,[1] and particularly metal-containing discotics,[2] underscore our belief that complementary new classes of engineering materials will originate from among these types of liquid crystals. Certainly, the extremely anisotropic and order-dependent nature of the elastic moduli, strengths, and thermal conductivities of these materials[3] has attracted interest from a rheological and mechanical standpoint. In addition, the ordered aromatic systems display unusually large and anisotropic charge carrier mobilities,[4] making them particularly attractive in the areas of photoconductivity and stimulated emission. Addition of metal ions, particularly paramagnetic centers, to related organic systems offers the possibility[5] of dramatically altering the responsiveness of these materials to applied magnetic fields.

Magnetic alignment stands as potentially the most straightforward and efficient means to produce molecular materials ordered over bulk length scales. The coupling energy between an isolated anisotropic molecule and an applied magnetic field, **H**, is insignificantly small relative to thermal energy in almost all circumstances. Rather, molecular alignment in liquid crystals is a domain phenomenon, with an effective coupling energy on the order of $^1/_2N(\Delta\chi)\mathbf{H}^2$, where $\Delta\chi$ is the magnetic polarization and N is the number of molecules in a domain. Specifically, the free energy of alignment of such a system can be expressed[6] as $\Delta G_{\text{align}} = -^1/_2(\Delta\chi)(\mathbf{H}\cdot\mathbf{n})^2$. This formulation emphasizes the importance of the orientation of the molecular director, **n**, with respect to the applied magnetic field. In addition to the simple summation effect of correlation of molecular

* To whom correspondence should be addressed.

† Portions of this work were presented at the August 2000 meeting of the American Chemical Society, ACS abstract 220: 491-INOR, part 1, 2000.

‡ Department of Chemistry, Indiana University.
§ Korea Advanced Institute of Science and Technology.
|| National Institute of Standards and Technology.
⊥ Department of Physics, Indiana University.
The Ohio State University.

(1) Serrano, J. L., Ed. *Metallomesogens*; VCH Publishers: Weinheim, 1996.

(2) Boden, N.; Bushby, R. J.; Clements, J.; Movaghar, B. *J. Mater. Chem*. **1999**, *9*, 2081. Cammidge, A. N.; Bushby, R. J. *Handbook Liq. Cryst*. **1998**, *2B*, 693.

(3) Hurt, R. H.; Chen, Z.-Y. *Phys. Today* **2000**, *53*, 39. Singh, K.; Pandey, N. S. *Liq. Cryst*. **1998**, *25*, 411. Wang, L.; Rey, A. D. *Liq. Cryst*. **1997**, *23*, 93. Chisholm, M. H.; Mackley, M. R.; Marshall, R. T. J.; Putilina, E. F. *Chem. Mater*. **1995**, *7*, 1938. Hammouda, B.; Mang, J.; Kumar, S. *Phys. Rev. E* **1995**, *51*, 6282. Mang, J. T.; Kumar, S.; Hammouda, B. *Europhys. Lett*. **1994**, *28*, 489.

(4) Palenberg, M. A.; Silbey, R. J.; Malagoli, M.; Bedas, J.-L. *J. Chem. Phys*. **2000**, *112*, 1541. Monobe, H.; Mima, S.; Shimizu, Y. *Chem. Lett*. **2000**, *9*, 1004. Van De Craats, A. M.; Warman, J. W.; Fechtenkotter, A.; Brand, J. D.; Harbison, M. A.; Mullen, K. *Adv. Mater*. **1999**, *11*, 1469. Nakayama, H.; Ozaki, M.; Schmidt, W. F.; Yoshino, K. *Jpn. J. Appl. Phys., Part 2* **1999**, *38* (9A/B), L1038. Bacher, A.; Bleyl, I.; Erdelen, C. H.; Etzbach, K. H.; Haarer, D.; Paulus, W.; Schmidt, H.-W. *Polym. Mater. Sci. Eng*. **1999**, *80*, 250. Bleyl, I.; Erdelen, C.; Schmidt. H.-W., Haarer, D. *Philos. Mag. B* **1999**, *79*, 463.

(5) Ikeda, S.; Takanishi, Y.; Ishikawa, K.; Takezoe, H. *Mol. Cryst. Liq. Cryst*. **1999**, *329*, 589. Hare, B. J.; Prestegard, J. H.; Engelman, D. M. *Biophys. J*. **1995**, *69*, 1891.

(6) Dekker: A. J. *Can. J. Phys*. **1987**, *65*, 1185. Maier, W.; Saupe, A. *Z. Naturforsch., A: Phys. Sci*. **1959**, *14*, 882.

10.1021/cm010428c CCC: $22.00
Published on Web 03/30/2002

anisotropies, aggregation within domains clearly also has the potential to alter the orientation of **n**.

To account for their ferromagnetism and antiferromagnetism,[7−9] π-stacking-induced spin polarization and intermolecular nitrogen-metal superexchange pathways have been invoked for molecular materials based on the porphyrin and tetraazaporphyrin ring systems.[9] Such structurally based issues are difficult to address for many of these materials because of their propensity to crystallize as thin fibers. In general, slipped ring (ring-tilted) columnar structures are common among aromatic molecular materials.[10] While unsubstituted aromatics[11] generally form herringbone-like structures which allow for CH$-\pi$ intermolecular interactions, alkyl-substituted aromatics[12] generally aggregate with the molecular ring planes of adjacent columns parallel to one another (although still with slipped rings). The few crystallized thioalkyl-substituted derivatives[13] all form herringbone-like structures in which metal−sulfur intermolecular interactions play an important role. The ring tilt has been found to persist in the mesophases of some of the liquid-crystalline derivatives.[14]

We describe herein our studies of the condensed phase structures, in the presence and absence of applied magnetic fields, of a series of metalloporphyrazine liquid crystals. We have found that, for the most part, these molecular materials (Scheme 1, where M = Co, Ni, or Zn) exhibit distinct long-range magnetic alignment, which is of fundamental importance in determining the physiochemical properties dictating potential materials applications. To our knowledge, this is the first study using diffraction methods of the magnetic alignment of metal-containing discotic liquid crystals.

Experimental Section

The investigated metalloporphyrazines, hereafter abbreviated as MS10 for a particular metal M, were prepared using a synthesis described previously in some detail,[15] which relies upon earlier methodology.[16] The materials employed in this study were purified by recrystallization from chilled hexanes. Purities were confirmed by ^{1}H- and ^{13}C{^{1}H}-NMR spectroscopy, LDI- and FAB-MS, and elemental analysis (see Supporting Information). The preparations and nomenclature are summarized in Scheme 1. Note that synthesis of these octa-substituted porphyrazine derivatives is remarkably inexpensive relative to the analogous porphyrins, proceeding through straightforward organic substitution chemistry and a metal-templated cyclization.

Scheme 1. Preparation and Nomenclature of the Studied Alkylthio-Substituted Porphyrazine Metallomesogens

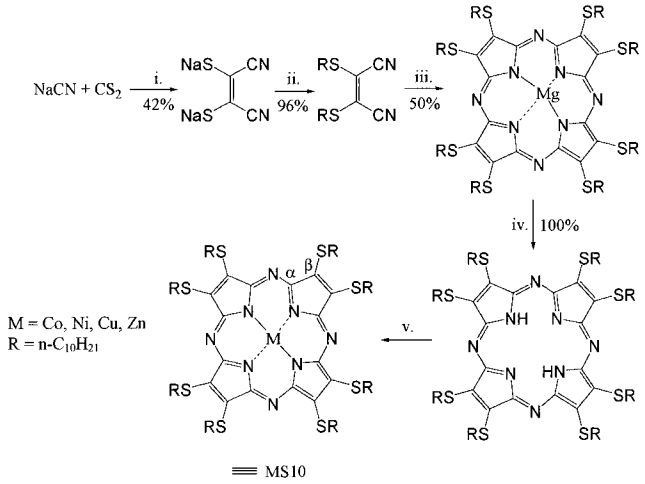

^{13}C labeling was introduced through the use of 99% ^{13}C-enriched NaCN purchased from Cambridge Isotope Laboratories, Inc. Apart from reduced scale (1.0 g of Na^{13}CN), the synthetic procedure employed to obtain these labeled derivatives was identical to that described above. The following mean yields were achieved per a preparative step: $Na_2S_2C_2(CN)_2$, 40%; $(H_{21}C_{10}S)_2C_2(^{13}CN)_2$, 97%; $S10H_2$, 54%. Metal substitution was in all cases virtually quantitative. LDI-MS revealed ^{13}C enrichment of 99% at the α position of each of the metalloporphyrazine products.

Differential scanning calorimetry was performed using a DuPont Instruments 910 DSC interfaced with a Thermal Analyst 2100 processing unit. Temperatures and enthalpies were calibrated to an indium standard.

Polarized optical microscopy was performed using an Olympus BX60 polarizing light microscope in transmitted light mode equipped with a Linkam LTS 350 hot stage and a Sony DXC-970MD 3CCD color video camera.

Fluid NMR spectra were collected on a Varian Unity Inova spectrometer (^{13}C Larmor frequency = 100 MHz) and Gemini 2000 (^{13}C Larmor frequency = 75 MHz) spectrometers. Samples were loaded into high-resolution Wilmad NMR tubes as virgin (solution-crystallized) powders. They were heated to their isotropic phases and then cooled to the temperature of interest within the NMR probe. The spectra were referenced to an external chloroform standard, contained in a separate NMR tube.

Solid state NMR spectra were obtained on a Bruker Avance DSX spectrometer. Samples were loaded to ceramic sample holders as finely ground virgin powders. Annealed samples were obtained by heating outside of the spectrometer to the isotropic phase for 0.5 h and cooling at a rate of 1 °C/min, followed by grinding to a fine powder. Cross polarization magic-angle spinning (CP-MAS) solid state NMR spectra were collected at spinning speeds of 2−8 kHz. A dipolar dephasing delay of 100 μs following the contact time of the cross polarization was applied in some cases to edit the methylene

(7) Yee, G. T.; Korte, B. J.; Sellers, S. P.; Reiff, W. M.; Frommen, C. M. *Mol. Cryst. Liq. Cryst.* **1999**, *335*, 23 and references therein. Sellers, S. P.; Korte, B. J.; Nakajima, S.; Iijima, Y. (Ricoh Co., Ltd., Japan). Jpn. Kokai Tokkyo Koho 96-255467, 1998. Kajiwara, A.; Takamizawa, S.; Yamaguchi, T.; Mori, W.; Yamaguchi, K.; Kamachi, M. *Mol. Cryst. Liq. Cryst. Technol. Sec. A* **1997**, *306*, 25. Iijima, Y.; Nakajima, S. (Ricoh Co., Ltd., Japan). Jpn. Kokai Tokkyo Koho 96-139338, 1997. Nakajima, S.; Gegorian, L. Jpn. Kokai Tokkyo Koho 96-63688, 1997. Nakajima, S. Jpn. Kokai Tokkyo Koho 95-350524, 1997. Reoniido, G.; Yakushi, H. Jpn. Kokai Tokkyo Koho 95-47859, 1996. Shimizu, Y.; Miya, M.; Nagata, A. Eur. Pat. Appl. 95-301945, 1995.

(8) Ricciardi, G.; Bencini, A.; Bavoso, A.; Rosa, A.; Lelj, F. *J. Chem. Soc., Dalton* **1996**, 3243.

(9) Sellers, S. P.; Korte, B. J.; Fitzgerald, J. P.; Reiff, W. M.; Yee, G. T. *J. Am. Chem. Soc.* **1998**, *120*, 4662. Barraclough, C. G.; Martin, R. L.; Mitra, S. *J. Chem. Phys.* **1970**, *53*, 1638.

(10) Scheidt, W. R.; Lee, Y. J. *Struct. Bonding* **1987**, *64*, 1.

(11) McKeown, N. B. *Phthalocyanine Materials*; Cambridge University Press: Cambridge, 1998 and references therein. Cox, E. G.; Cruickshank, W. J.; Smith, J. A. S. *J. Chem. Soc.* **1958**, *247*, 1. Robertson *Proc. R. Soc. London, Ser. A* **1951**, *207*, 101.

(12) Brown, S. P.; Zhu, X. X.; Saalwächter, K.; Spiess, H. W. *J. Am. Chem. Soc.* **2001**, *123*, 4275. Ochsenfeld, C.; Brown, S. P.; Schnell, I.; Gauss, J.; Spiess, H. W. *J. Am. Chem. Soc.* **2001**, *123*, 2597. Brown, S. P.; Schnell, I.; Brand, J. D.; Mullen, K.; Spiess, H. W. *J. Mol. Struct.* **2000**, *521*, 179. Scheidt, W. R.; Turowska-Tyrk, I. *Inorg. Chem.* **1994**, *33*, 1314.

(13) (a) Ricciardi, G.; Rosa, A.; Ciofini, I.; Bencini, A. *Inorg. Chem.* **1999**, *38*, 1422. (b) Ricciardi, G.; Bavoso, A.; Bencini, A.; Rosa, A.; Lelj, F.; Bonosi, F. *J. Chem. Soc., Dalton Trans.* **1996**, 2799.

(14) Morelli, G.; Ricciardi, G.; Roviello, A. *Chem. Phys. Lett.* **1991**, *185*, 468. André, J.-J.; Bernard, M.; Piechocki, C.; Simon, J. *J. Phys. Chem.* **1986**, *90*, 1327.

(15) Lelj, F.; Morelli, G. Ricciardi, G.; Roviello, A.; Sirigu, A. *Liq. Cryst.* **1992**, *12*, 941.

(16) Doppelt, P.; Huille, S. *New J. Chem.* **1990**, *14*, 607. Schramm, C. J.; Hoffman, B. M. *Inorg. Chem.* **1980**, *19*, 383.

resonances. Peak fitting and Hertzfeld−Berger spinning sideband analyses[17] were performed with the Bruker Xedplot software package.

Discrete X-ray diffraction data were obtained with a Scintag XDS 2000 $\theta-2\theta$ goniometer employing Cu Kα radiation. It was equipped with a specially machined copper block and cartridge heater assembly regulated with an Omega CN132 Temperature/Process Controller. Samples were loaded as finely ground solution-crystallized powders to silver or aluminum pans. Annealed samples were prepared in a manner analogous to that described above for solid state NMR experiments. The source current and voltage were regulated at 35 mA and 40 kV. Monochromatic radiation was obtained by employing a graphite filter on the diffracted beam and the X-rays were detected with a NaI scintillation detector. Peak widths were corrected for instrumental resolution. Pattern indexing was performed with the JADE MDI software package. We emphasized the first eight diffraction peaks (2 Å < 10°) in our indexing procedures.

Neutron scattering data were collected at the NIST Center for Neutron Research (NCNR), Gaithersburg, MD, using the NG3 small-angle neutron scattering (SANS) beamline. Neutrons with a wavelength, λ, of 4.32 Å and full-width-at-half-maximum $\delta\lambda/\lambda$ of 0.30 were collimated using a source aperture of 5.00 cm and a sample aperture of 1.27 cm. The distance between these aperatures was 3.37 m. The scattering intensity was measured using a 2D detector as a function of **q**, the scattering vector, where $|\mathbf{q}| = 4\pi \sin(\theta)/\lambda$ and 2θ is the scattering angle. The sample-to-detector distance was 1.86 m. Intensity data were corrected for environmental scattering, detector dark current, and nonuniformities of the detector. Samples were loaded in their isotropic phases to a copper-supported quartz cell with a 1.0-mm path length. The sample temperature was regulated to within 1 °C through the copper support. A figure of this cell and of the experimental geometry is included in the Supporting Information. The sample cell was placed between the poles of an electromagnet, which provided a field of up 1.22 T at the interrogation spot, as measured using a gaussmeter. The field vector was perpendicular to the neutron beam.

Results and Discussion

Investigations of these metalloporphyrazine liquid crystals by differential scanning calorimetry and polarized optical microscopy have been reported,[15] as have the X-ray scattering patterns of the mesophases. The assigned structure consists of hexagonal arrays of disordered columns. The measured phase transitions occur at quite accessible temperatures (all <200 °C). Our measurements confirm these previously reported results, as summarized in the Supporting Information.

Diffraction Studies of Phase Behavior. The X-ray diffraction data described in this section have been tabulated in the Supporting Information. The diffraction pattern of NiS10, as crystallized from solution, may be indexed to a *P*2(3) space group. The pattern changes markedly upon annealing, such that the new monoclinic space group is *P*21(4). These diffraction patterns are presented in Figure 1. The space group of the other derivatives is not affected by annealing. Microcrystalline CuS10 and ZnS10 share the same space group as the solution-crystallized NiS10, while the space group of CoS10 is the same as the annealed nickel complex. None of these microcrystalline samples is particularly well-ordered, and the consequent limited number of reflections limits our ability to draw detailed structural conclusions. The mechanism of crystal growth does not affect the correlation lengths in any systematic manner.

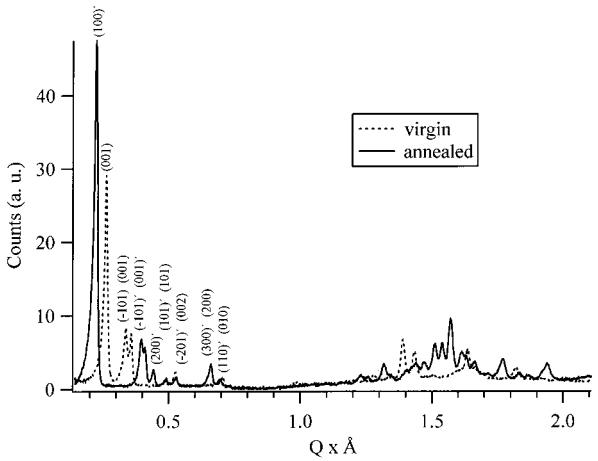

Figure 1. Powder X-ray diffraction patterns of NiS10, as crystallized from hexane solutions ("virgin") and after annealing and slow cooling from the isotropic phase. The patterns have been indexed to *P*2(3) and *P*21(4) monoclinic space groups, respectively.

The intense primary reflection of these solids, which occurs at particularly small angles, makes them especially amenable to small-angle scattering studies. Reflections in this region, in a general sense only and based on assignments of diffraction patterns of the liquid-crystalline phase, are attributed to the intercolumnar lattice.

Intense reflections in the intercolumnar region were also observed by neutron scattering. To demonstrate the origin of the neutron scattering contrast within the sample, this sample may be approximated as a two-phase system consisting of (1) the fairly rigid metalated porphyrazine rings and (2) the more flexible thioalkyl chains. As a simple model the porphyrazine ring may be represented as an inner discoid surrounded by a cylindrical thioalkyl sheath. From previous X-ray crystallographic data[13] the inner diameter is 8.3 Å. On the basis of the mesophase X-ray powder data cited above, the outer diameter is 26.0 Å and the thickness is 4.3 Å. The resulting volume of the porphyrazine disks is 200 Å^3 and that of the chains is 2100 Å^3. Employing these volumes and a collection of standard neutron scattering lengths,[18] we use the standard equation

$$|\Delta\rho|^2 = (\rho_{\text{core}} - \rho_{\text{shell}})^2$$

to calculate a scattering contrast, $|\Delta\rho|^2$, which ranges from 9.1 to 9.9 × 10^{29} m^{-4} depending on the metal center (lowest for Co and highest for Ni). This is a high value for the contrast and is consistent with the intense reflections that were observed.

The SANS patterns of NiS10, as obtained upon cooling from the isotropic phase at 5 °C/min, are presented in Figure 2. The observations described here apply generally for all the investigated MS10 derivatives. Upon cooling through the liquid-to-liquid-crystalline phase transition, the *Q* value of the primary observed reflection discontinuously decreases and the correlation length of the intercolumnar lattice increases markedly. A further ordering occurs during the transition from this hexagonal liquid-crystalline phase to the

(17) Herzfeld, J.; Berger, A. E. *J. Chem. Phys.* **1980**, *73*, 6021.

(18) Sears, V. F. *Neutron News* **1992**, *3*, 29. http://www.ncnr.nist.gov/resources.

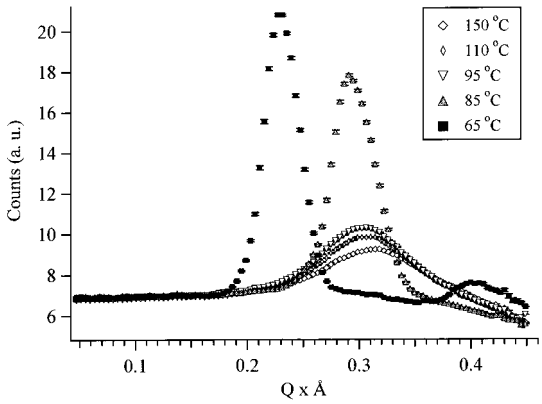

Figure 2. Small-angle neutron scattering patterns of NiS10 collected during cooling from the isotropic phase. The patterns upon heating are identical.

monoclinic crystalline phase. These phase characteristics are enantiotropic: apart from a small hysteresis, the transition temperatures and correlation lengths are the same during the reheating process. Through all phases, the *Q* values of these reflections are very close to those observed in the X-ray experiments, confirming the length scales employed in the core/shell model of the scattering. The solid-state SANS patterns of these samples also confirm the difference in space group between the Cu, Zn and the Ni, Co annealed derivatives. The peak positions are summarized in the Supporting Information.

Diffraction Studies of Magnetic Response. Upon cooling into the liquid-crystalline phase in the presence of an applied magnetic field on the order of 1 T, a significant induced anisotropy in the measured small-angle area neutron diffraction pattern develops for the Co, Ni, and Zn derivatives. The anisotropic diffraction pattern of CoS10 is depicted in Figure 3. Diffraction intensity is strongest along the applied field vector and weakest perpendicular to the field. This places the intercolumnar lattice directly along the field vector and the columnar directors themselves perpendicular to it, as depicted in the Figure 3 inset.

The anisotropy of the pattern clearly increases with decreasing temperature within the liquid-crystalline phase, as depicted in Figure 4a. To attain these data, the material (CoS10, in this case, although the discussion applies generally) was first heated, in the absence of an applied magnetic field, to a temperature well into its liquid phase, at which point the diffraction pattern was confirmed to be isotropic. The field was then set to the desired strength and the material cooled at approximately 5 °C/min, with 15-min pauses for equilibration and data collection every 20 °C (5 °C for NiS10 and ZnS10 since the liquid-crystalline temperature regions are smaller in these cases). The sample was allowed to attain thermal equilibrium at each temperature, as judged by the lack of change of the pattern at a particular temperature over multiple 5-min data collections. Thermal gradients were very small across the sample since coexisting phases were not detected, even when monitoring at 1 °C intervals.

Magnetic alignment, once induced during cooling within the applied magnetic field, is locked and field-independent: removal of the field within the mesophase temperature region resulted in no measurable change in the diffraction pattern over several hours, suggesting at least a very long relaxation time of the induced domain alignment. Alignment is preserved in the cooled solids, which as previously noted have different lattice structures (monoclinic instead of hexagonal) than the liquid crystals. An unchanged diffraction pattern was measured after allowing the cooled solid to stand in the absence of an applied magnetic field for 24 h.

A number of magnetic field strengths were tested during the cooling process of each material. As depicted in Figure 4b, the growth of the diffraction anisotropy for CoS10 is apparent at fields as low as 0.25 T, and it becomes increasingly well-defined as the field strength is increased to 0.52 T. At higher fields the degree of alignment begins to reach a plateau, continuing to increase more gradually to 0.89 T. The threshold aligning field may be defined as the field strength beyond which the diffraction anisotropy begins to plateau. On the basis of this rough and arbitrary measure, it is however clear that the threshold aligning field for CoS10 is approximately half that of ZnS10 or NiS10. The threshold aligning fields of the latter complexes are about 1.2 T. Only a small degree of increased alignment over that seen with a 1.2-T applied field was noted when cooling a sample of NiS10 in a field of 9.40 T. While induced diffraction anisotropy of CoS10 is first apparent at a field strength of 0.25 T, induced anisotropy of the diffraction patterns of NiS10 and ZnS10 is not apparent until a field of 0.5 T is applied. For CuS10, no induced diffraction anisotropy was detected, even employing fields as high as 1.02 T.

In short, the data presented above allow us to conclude that ease of magnetic alignment for this series decreases according to the following trend: CoS10Pz > ZnS10Pz ∼ NiS10Pz > CuS10Pz. This matches the result that we had predicted a priori on the basis of the competing diamagnetic and paramagnetic moments of these systems. The diamagnetic moment of porphyrinoid rings is large and anisotropic. The ring current effect leads to a diamagnetic repulsion that is significantly greater along the ring director than within the ring plane. Thus, an isolated diamagnetic porphyrazine molecule would have a small tendency to align such that its ring plane was parallel to an external magnetic field. However, the tendency of isolated molecules to orient in applied magnetic fields is small, else we might expect to see anisotropic diffraction within the liquid phase. We must therefore consider the anisotropy of each domain as a whole. Within the structure that has been posited for the liquid-crystalline phase, the ring directors lie at an angle of approximately 30° from the directors of the columns that contain them (see NMR studies, below). Since no evidence indicates a preferred tilt direction of the rings, the resultant diamagnetic moment of the domain is most repulsive parallel to its columnar directors. Thus, the columns align with their directors perpendicular to the applied magnetic field.

The other two metal derivatives have paramagnetic moments that must be considered in addition to their diamagnetic moments.[19] In the case of Co, with a 2+ oxidation state and a square-planar ligand geometry in these systems, the unpaired electron resides in a d(z^2) orbital.[20] Mixing in of energetically low-lying excited

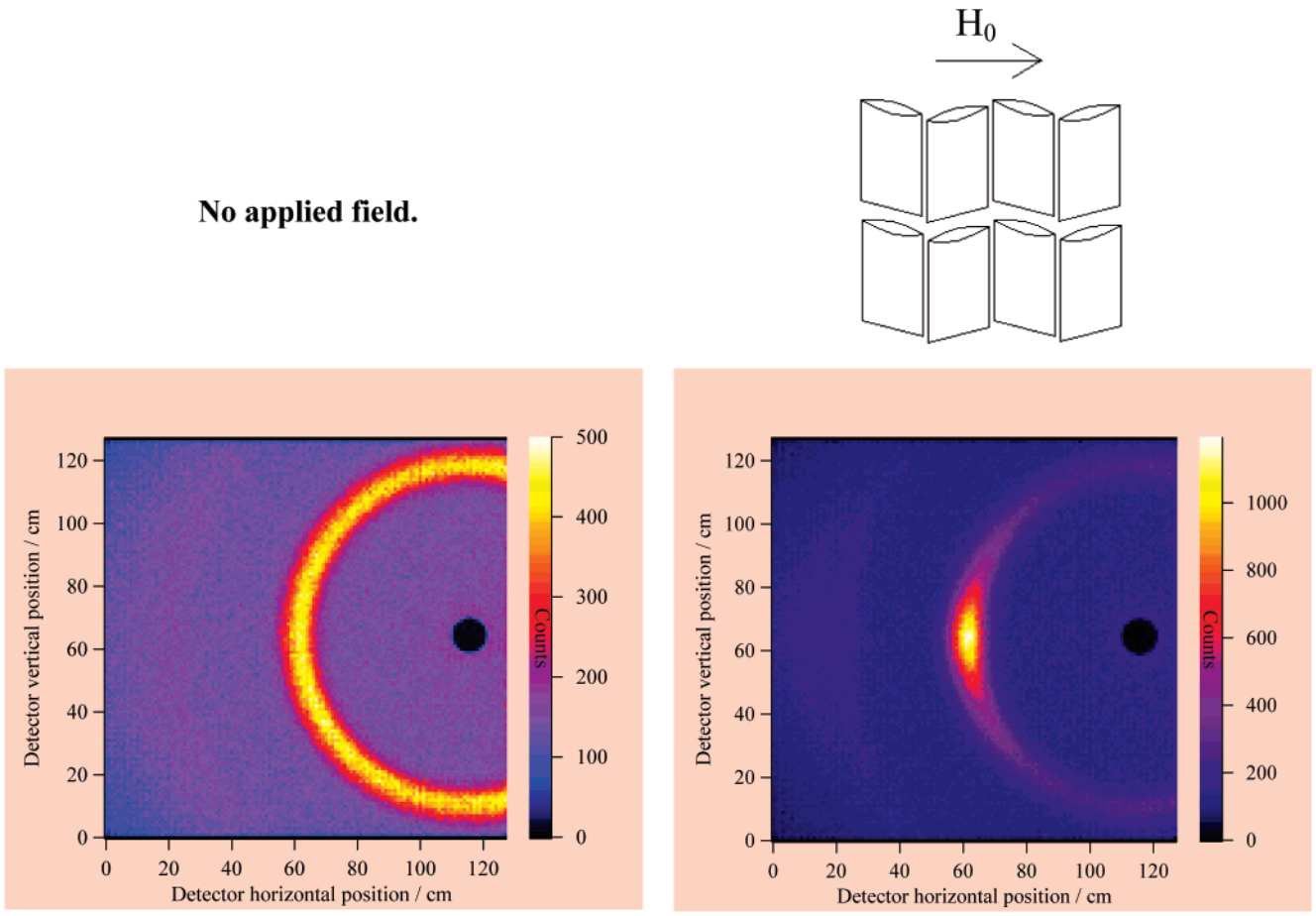

Figure 3. Area SANS patterns of CoS10 in its solid state, after cooling in the absence of an applied field (left) and after cooling through a 1.02-T magnetic field (right). The applied field (H_0) direction and corresponding columnar alignment for the latter case are depicted.

states that contain an unpaired electron in the d(xz, yz) orbital set leads to a paramagnetic moment directed in the x,y (ring) plane. This enhances the tendency of the ring planes to align parallel to the applied magnetic field, and thus leads to a greater ease of alignment of the columnar directors perpendicular to the applied field.

The Cu system, on the other hand, has its unpaired electron in a d(x^2-y^2) orbital. Mixing in of an energetically low-lying excited state with the unpaired electron in a d(xy) orbital leads to a paramagnetic moment which is directed along the z molecular axis. This opposes the diamagnetic alignment tendency of the molecule and of the system. In this particular case, the diamagnetic and paramagnetic moments are of comparable magnitude, frustrating any sort of domain alignment.

^{13}C NMR Studies. ^{13}C NMR measurements provide additional evidence for the magnetic alignment of the diamagnetic derivatives. The solid state ^{13}C NMR data are collected in Table 1. The CP-MAS and static spectra are complicated by the occurrence of multiple carbon resonances for the solution-equivalent α sites. The nonequivalence of these sites in the solid state, and their clustering into two primary groups, is consistent with the slipped ring structure. An obvious feature of these data is the fact that one chemical shift tensor element, δ_{33}, is shifted upfield with respect to the other two. For analogous aromatic systems, based on single-crystal experiments and theoretical studies, δ_{33} has been found to be directed perpendicular to the ring plane and its marked upfield shift attributed to aromatic ring current effects.[21] This designation places δ_{11} and δ_{22} within the ring plane.

Table 1. Solid State NMR Parameters: Mean Values for the α Carbons

parameter	NiS10	ZnS10	parameter	NiS10	ZnS10
δ_{iso}/ppm	149	154	δ_{11}/ppm	217	215
Δ_{CS}/ppm	95	87	δ_{22}/ppm	176	181
η	0.42	0.40	δ_{33}/ppm	53	67

The magnetic alignment of these materials may be addressed through an examination of the fluid ^{13}C NMR spectra of the neat metalloporphyrazines. Figure 5

(19) Previous electronic structure calculations and experimental data have demonstrated that, in almost all cases, the ground state of cobalt porphyrinoid derivatives has mostly metal d(z^2) character.[13a] Thiolate peripheral substitution tends for isolated molecules to energetically slightly favor (by 0.1 eV) electronic ground states with minimal d(z^2) character.[13a] However, axial M−S intermolecular interactions present in these systems in the neat condensed phases disturb the energetics of the isolated molecules significantly, such that the ground state almost surely once again has predominantly d(z^2) character.

(20) For a general discussion, see Drago, R. S. *Physical Methods for Chemists*, *2nd ed.*; Saunders College Publishing: Ft. Worth, 1992; p 567.

(21) Strohmeier, M.; Orendt, A. M.; Facelli, J. C.; Solum, M. S.; Pugmire, R. J.; Parry, R. W.; Grant, D. W. *J. Am. Chem. Soc.* **1997**, *119*, 7114. Veeman, W. S. *Prog. Nucl. Magn. Reson. Spectrosc.* **1984**, *16*, 19.

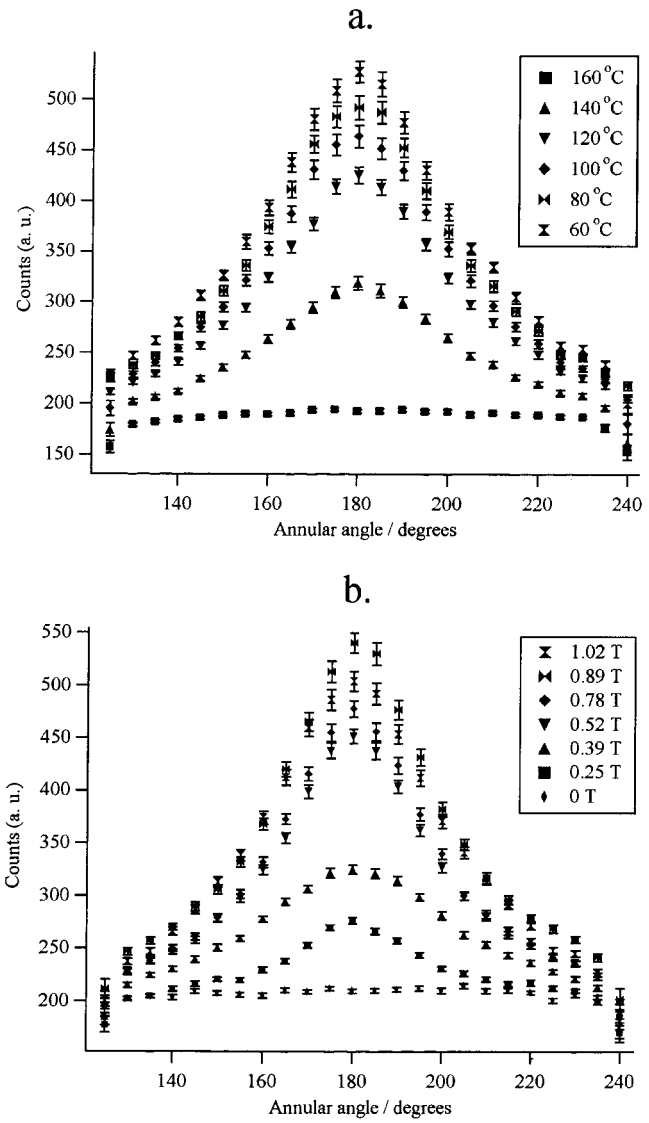

Figure 4. Plots of the SANS intensity at $Q = 0.291$ versus annular angle about the diffraction ring for CoS10. The peak maximum of the aligned mesophase falls at 180°, indicating orientation of the intercolumnar lattice along the magnetic field vector as in Figure 3. Plot (a) depicts the temperature dependence of the diffraction anisotropy at a fixed applied magnetic field of 1.02 T. Plot (b) depicts the diffraction anisotropy induced as the sample was cooled through different applied magnetic fields to a fixed temperature of 80 °C.

depicts the fluid spectra of the ^{13}C-labeled ZnS10 derivative obtained during cooling at 5 °C/min from the isotropic phase. At 90 °C, in the isotropic liquid phase, the labeled carbons give rise to a relatively sharp resonance. Here, as in typical solution state NMR spectra, broadening anisotropic interactions are averaged by rapid isotropic molecular tumbling. At 75 °C the growth of the liquid-crystalline phase is apparent, as a distinct signal develops. At 50 °C this phase occupies the entire sample space of the NMR tube. It is particularly relevant that the signal associated with the mesophase is broadened and shifted downfield relative to the same site in the liquid phase.

To account for the noted downfield shift, a reconsideration of the ^{13}C NMR spectra of the neat powders is in order. Note that the position of the isotropic shift of the powder and liquid are virtually identical, indicating

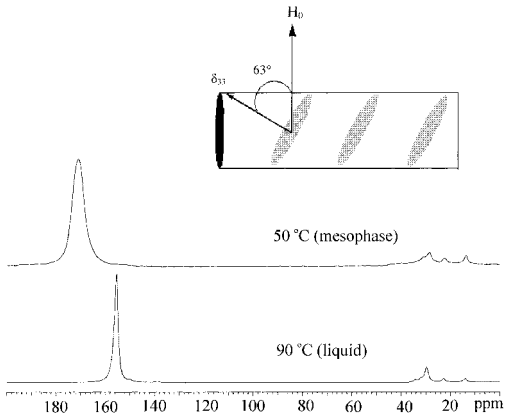

Figure 5. ^{13}C NMR spectra of neat ZnS10, labeled at the α ring site, during cooling from the isotropic phase. Inset: Model of the intracolumnar magnetic alignment of this system. The porphyrazine ring perpendiculars have a time-averaged effective angle of 63° with respect to the magnetic field vector and 27° with respect to the columnar directors.

that the chemical environments of the α carbons in these two phases are similar. It thus seems highly unlikely that the noted differences in chemical shift between the liquid and liquid-crystalline phases can be explained on the basis of differences in chemical environment. Rather, the noted chemical shift difference must be attributable primarily to anisotropic molecular alignment with respect to the magnetic field of the spectrometer. Such anisotropic NMR spectra are well-precedented[22] in liquid-crystalline phases.

For these planar aromatic molecules with virtual D_{4h} symmetry, an axially symmetric chemical shift tensor coincident with the axes of molecular symmetry may be assumed. δ_{aniso}, the displacement of the chemical shift from its isotropic value, can then be written[23] in terms of $\Delta\delta = \delta_{||} - \delta_{\perp}$ as

$$\delta_{aniso} = \frac{2}{3} S \Delta\delta$$

so that

$$\delta_{obs} = \delta_{iso} + \delta_{aniso} = \delta_{iso} + \frac{2}{3} S \Delta\delta$$

Here, S is an order parameter, varying between -0.5 and 1.0 for orientations of δ_{33} perfectly perpendicular and parallel to the applied magnetic field vector. δ_{obs} is the observed chemical shift in the liquid-crystalline phase and δ_{iso} is the isotropic shift. S implies a time-averaged effective angle of the molecular director with respect to the applied magnetic field such that

$$S = \left\langle \frac{3\cos^2\theta - 1}{2} \right\rangle$$

Applying such analysis to the powder-derived directional elements of the chemical shielding tensor for

(22) Doug, R. Y. *Nuclear Magnetic Resonance of Liquid Crystal, 2nd ed.*; Springer-Verlag: New York, 1997. Sanders, C. R., II; Hare, B. J.; Howard, K. P.; Prestegard, J. H. *Prog. Nucl. Magn. Reson. Spectrosc.* **1994**, *26*, 421. Emsley, J. M.; Lindon, J. C. *NMR Spectroscopy Using Liquid Crystalline Solvents*; Pergamon Press Ltd.: Oxford, 1975.

(23) Cowan, B. *Nuclear Magnetic Resonance and Relaxation*; Cambridge University Press: Cambridge, 1997.

Table 2. Fluid NMR Parameters

parameter	NiS10	ZnS10	parameter	NiS10	ZnS10
δ_{soln}/ppm	148.9	156.2	S_{lc}	0.19	0.18
δ_{liq}/ppm	147.3	155.5	θ_{lc}	63°	62°
δ_{lc}/ppm	167.1	169.8			

these complexes allows for calculation of the order parameters and time-averaged effective angles (θ) listed in Table 2. The latter are on the order of 63° and clearly lead to a disfavoring of δ_{33} and consequent downfield shift of the carbon resonance in the anisotropic fluid phase. The nature of the metal (M = Ni or Zn) appears to have a negligible effect on the liquid-crystalline alignment disorder.

Disorder is clearly a relative term—the above refers to disorder relative to perfectly parallel ring *z*-axis orientation with respect to the applied magnetic field. Recalling the commonly observed tilt angle within the known crystal structures of closely analogous materials, an active role of the domain structure in determining the effective ring angle may be supposed. Whatever the case, an orientation of the columnar directors perpendicular to the applied magnetic field may be anticipated, as depicted in Figure 5 (inset) and as confirmed by our SANS studies.

A further confirmation of these results is available through investigation of the static solid state ^{13}C NMR spectra of the aligned materials. Spectra of ZnS10 cooled at 5 °C/min with applied fields of 0 and 9.40 T are presented in the Supporting Information. While considerable disorder remains in the aligned sample, it is clear that the data reveal a decreased population of labeled nuclei with their *z* chemical shift tensors parallel to the applied field. The population of nuclei with δ_{11} parallel to the applied field is also decreased somewhat, lending support to the idea of disk tilting. We have not yet undertaken a more quantitative assessment of these aligned solid state spectra.

Conclusions

The MS10 solids crystallize from solution and the mesophase in monoclinic cells with space group *P*2(3) or *P*21(4). Only the larger metal centers (Co, Ni) adopt the latter space group, which for nickel is favored by annealing.

Domain growth with a preferred orientation is observed in the presence of an applied magnetic field of ca. 0.5 T or greater for the diamagnetic derivatives. This locked alignment becomes increasingly uniform at lower temperatures within the mesophase. It is also more uniform at higher applied fields and is maintained in the solid state. The liquid-crystalline columns align perpendicular to applied magnetic fields, and the porphyrazine rings exhibit a time-averaged effective ring tilt angle of ca. 63° with respect to the field vector. The threshold aligning field for the cobalt derivative is half that of the diamagnetic derivatives, whereas the copper derivative exhibits no alignment at an applied magnetic field of 1 T. We are actively exploring the dynamics of this system.

Acknowledgment. We thank the National Science Foundation and The Ohio State University for financial support and the reviewers for their constructive comments concerning the presentation of this work. For the work at NIST, this material is based upon activities supported by the National Science Foundation under Agreement No. DMR-9986442. The work of S.-M.C. is supported by the Ministry of Information and Communication of Korea through Contract No. IMT 2000-B3-2. We also thank Steven R. Kline for helpful technical assistance.

Supporting Information Available: Samples characterization data and figures and tables. This material is available free of charge via the Internet at http://pubs.acs.org.

CM010428C